On the Chemical Bonding in the Intermetallic B32-Type Compounds LiMe

(Me = Al, Zn, Ga, Cd, and In)

P. C. Schmidt

Institut für Physikalische Chemie, Physikalische Chemie III, Petersenstr. 20, D-6100 Darmstadt, West Germany

Z. Naturforsch. **40 a**, 335 – 346 (1985); received January 29, 1985

Dedicated to Prof. Dr. Alarich Weiss on the Occasion of his 60th Birthday

The electronic charge distributions in the binary intermetallic B32 phases LiMe with Me = Zn, Cd, Al, Ga and In have been calculated by the relativistic augmented plane wave method. It is found that the character of the contribution from the various electron bands to the chemical bond is different for the lower valence bands and for the higher valence-conduction bands.

The lower valence bands are occupied by two electrons per formula unit LiMe and are predominantly of covalent s-p-type, formed by the diamond-like sublattice of the Me atoms. For all compounds the percentage p-like character is smaller than for the sp^3 hybrid within the molecular orbital picture. The valence bands above the covalent bands are s-p-like bands with enhanced metallic character.

Besides a large covalent contribution to the chemical bond in the intermetallic B32-type phases, a charge transfer from the lithium atoms to the IIb and IIIa elements is found. The amount of charge transfer is distinctly smaller than one electron per formula unit LiMe. It is shown that the charge transfer is correlated to the differences in the electronegativities of the corresponding atoms.

1. Introduction

Among the binary intermetallic compounds the Zintl phases which crystallize in the B32 type structure have some unusual physical properties. The B32 structure is a superstructure of the bcc lattice, where the nearest neighbours are four like and four unlike atoms (see Figure 1). The atoms are arranged in such a way that the atoms of the same kind form diamond-like sublattices. This arrangement suggests that for the AB compounds LiAl, LiGa and LiIn as well as for NaIn and NaTl, the B atoms build up closed valence subshells because of the transfer of a 4th electron from the alkali atoms [1–6]. In this case physical properties similar to those of semiconducting compounds should result. Indeed, the investigation of the magnetic properties (susceptibility and Knight shift) of B32 phases shows that large diamagnetic contributions to the susceptibility and Knight shift are present [7, 8], e.g. LiIn is diamagnetic [7]. Other physical properties, however, like the considerable range of homogeneity in the binary A-B systems (Na-Tl [9] or Li-Cd [10]) indicate a metallic structure [2]. The chemical bond in the B32 phases is described in the literature as metallic, covalent and ionic [11]. The stability and the chemical bond of these phases have been discussed in terms of the band structure as well as the atomic sizes, the atomic valence states and the differences in the electronegativities of the atoms

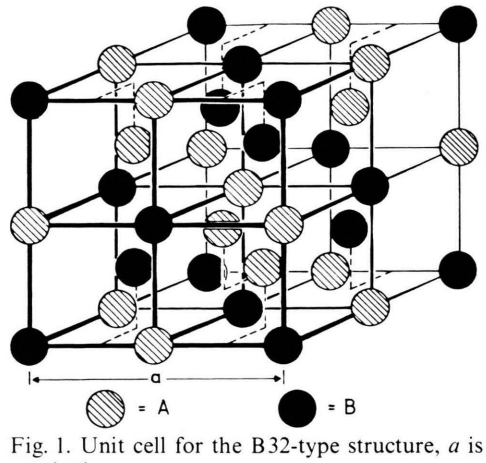

Fig. 1. Unit cell for the B32-type structure, *a* is the lattice constant.

Reprint requests to Dr. P. C. Schmidt, Physikalische Chemie I, Petersenstr. 20, D-6100 Darmstadt, West Germany.

0340-4811 / 85 / 0400-0335 $ 01.30/0. – Please order a reprint rather than making your own copy.

[1–4, 12–14]. It has already been pointed out that the sizes of the atoms A and B in the B32 phases AB should be identical [12, 14]. The aim of the present paper is to obtain some quantitative results for the interplay of the valence states and the electronegativities of the atoms and the chemical bond in the B32 phases.

To investigate trends in the physical behavior, the band structures and charge distributions of all known binary B32-phases LiMe are calculated. The charge transfer $\Delta Q = Q_m - Q_a$ in these phases is calculated by comparing the charge deduced from the band structure Q_m with the charge Q_a which one gets from overlapping atomic charge densities. ΔQ is correlated to differences in the electronegativities χ of appropriate valence electron configurations.

The values for χ from Pauling [15] are not very useful to study this correlation, because the differences in χ for the atoms Al, Ga and In are of the same order of magnitude as the accuracy of these values. Böhm and Schmidt [16], however, recently used a new theoretical method to calculate electronegativities for atomic valence configurations. This method is based on the density functional theory and gives the same trends in χ as found earlier from spectroscopic data [17]. Within this new method electronegativities of appropriate valence states can be calculated. To achieve this aim in the present work, valence electron configurations are deduced from the charge analysis of the band structure calculations, and for these valence configurations atomic electronegativities are calculated and the correlation to the calculated charge transfer ΔQ is studied.

The band structure calculations have been carried out by means of a relativistic augmented plane wave (RAPW) technique [18] using the muffin-tin approximation for the construction of the crystal potential and using the ansatz of the local electron density theory for the total energy [19–22]. A large amount of computer time is needed for a full self-consistent RAPW calculation. It is found, however, that for the investigation of the density of states and the charge analysis in the phases given above the simpler scalar RAPW (SRAPW) method [23] yields nearly the same results. Therefore all calculations of the present work are performed with this method. Within the relativistic SRAPW method the spin-orbit coupling is neglected and the spin has a good quantum number.

Band structure calculations for B32 phases have already been performed by the augmented plane wave method for LiAl, LiCd and LiZn [24], LiCd and LiIn [25], and for NaTl [12]. The main interest of these investigations was the determination of the density of states, the Knight shift and optical properties.

There exist also some investigations on the electronic band structure of B32-type phases by the pseudo-potential method [13, 14]. Especially the influence of like and unlike nearest neighbours on the electronic stability has been discussed. For this reason model calculations are performed in the present work and have been reported in the literature [12–14] for the B2 (CsCl type) structure. The B2-type structure has been chosen as the reference structure, as both structures, B2 and B32, are superstructures of the bcc lattice, and because in the CsCl structure all eight nearest neighbours are unlike atoms. In an earlier paper we have found [12] that for LiTl and NaTl the difference in the electronic ordering energy $\Delta E = E(\mathrm{B2}) - E(\mathrm{B32})$ is negative for LiTl and positive for NaTl, that is the valence electron energy favours the crystal structure found experimentally (B2 for LiTl and B32 for NaTl). In the present paper we have studied these differences in the ordering energy for the intermetallic systems LiMe.

2. Theory

Energy

On the basis of the relativistic version of the local density functional approach and of the muffin-tin model the total energy with frozen nuclei is given by [19–22]

$$E = T + U_{ee} + U_{en} + E_{xc} + E_{nn}\,; \tag{1}$$

$$T = \sum_{i=1}^{N} \langle \psi_i | \, (-i\,c\,\gamma\,\nabla + \tfrac{1}{2}\,c^2) \, | \psi_i \rangle\,; \tag{2}$$

$$U_{ee} = \int\int \frac{\varrho(\boldsymbol{r})\,\varrho(\boldsymbol{r}')}{|\boldsymbol{r}-\boldsymbol{r}'|}\,\mathrm{d}\tau\,\mathrm{d}\tau'\,; \tag{3}$$

$$U_{en} = -2\sum_{s} \frac{Z_s\,\varrho(\boldsymbol{r})}{|\boldsymbol{r}-\boldsymbol{r}_s|}\,\mathrm{d}\tau\,; \tag{4}$$

$$\varrho(\boldsymbol{r}) = \sum_{i=1}^{N} |\,\psi_i(\boldsymbol{r})\,|^2\,. \tag{5}$$

N is the number of electrons and Z_s is the nuclear charge. E_{nn} represents the nucleus-nucleus repulsion

and T is the sum of the kinetic and rest mass energy. The energy of the electron-electron repulsion is separated in two terms, the Coulomb term (3) and the exchange-correlation term E_{xc}. There are numerous approaches to expressions for E_{xc} in the literature [26–30]. In the present work we have used the relativistic exchange energy proposed by MacDonald and Vosko [22] and the correlation energy suggested by Vosko et al. [30] for all calculations.

The charge density ϱ, (5) is determined from the wave functions (4-spinors) ψ_i, which are solutions of the one-electron Dirac equations

$$[-i c \boldsymbol{\alpha} \nabla + \tfrac{1}{2} \beta c^2 + V(\boldsymbol{r})] \psi_i = \varepsilon_i \psi_i ; \tag{6}$$

$$V(\boldsymbol{r}) = \frac{\delta U_{ee}}{\delta \varrho} + \frac{\delta U_{en}}{\delta \varrho} + \frac{\delta E_{xc}}{\delta \varrho} . \tag{7}$$

The potential $V(\boldsymbol{r})$, (7) and the electrostatic energy U_{en} and U_{ee}, (3) are calculated on the basis of the muffin-tin approximation. The volume of the unit cell ω is separated in the volume of the non overlapping atomic spheres ω_s, $s = \text{Li, Al, ...}$, and the volume between the spheres ω' (see below Figure 8 a). The following three approximation are made for calculating $V(r)$, U_{en} and U_{ee}:

(a) The electron density in ω' can be approximated by a constant

$$\varrho_0 = Q'/\omega' , \tag{8}$$

where Q' is the electron charge in units of e^- inside the volume ω'.

(b) The electron charge density inside the muffin-tin spheres $\varrho(\boldsymbol{r})$ can be replaced by the spherical mean

$$\varrho_s(r) = \frac{1}{4\pi} \int\int \varrho(\boldsymbol{r}) \, \mathrm{d}\varphi \, \mathrm{d}\cos\vartheta . \tag{9}$$

(c) The distant terms are calculated by a procedure proposed by Slater and de Cicco [31].

Then one obtains for the energy

$$E = T + \sum_s \left(-8\pi \int_0^{R_s} Z_s r \, \varrho_s(r) \, \mathrm{d}r + \iint_{\omega_s} \frac{\varrho_s(r) \, \varrho_s(r')}{|\boldsymbol{r} - \boldsymbol{r}'|} \, \mathrm{d}\tau \, \mathrm{d}\tau' \right) + E_{xc} + C_{out} , \tag{10}$$

where the sum over the muffin-tin spheres represent the local Hartree energies inside the atomic spheres with radii R_s and the last term is a distant contribution, which one gets from the Ewald summation; for details see [12].

Using the one-electron equations (6), (10) can be rewritten in the form

$$E = \sum_i \varepsilon_i - \sum_s \iint_{\omega_s} \frac{\varrho_s(r) \, \varrho_s(r')}{|\boldsymbol{r} - \boldsymbol{r}'|} \, \mathrm{d}\tau \, \mathrm{d}\tau' + E'_{xc} + C'_{out} , \tag{11}$$

where E'_{xc} contains the exchange-correlation contribution and C'_{out} is a sum of distant terms, see [12].

On the basis of (11) the differences in the ordering energy between the B2 and B32 structure $\Delta E = E(\text{B2}) - E(\text{B32})$ can be approximated by the first term of this equation [12, 32, 33], that is by the differences of the sums of the one-particle energies. This method is analogous to the Hückel theory for π-electron systems. Taking only the first term of (11) for the valence electrons, ΔE can be expressed by integrals over the density of states $N(E)$:

$$\Delta E = E(\text{B2}) - E(\text{B32}) \approx \int_{E_{0,\text{B2}}}^{E_{F,\text{B2}}} N_{\text{B2}}(E) \, E \, \mathrm{d}E - \int_{E_{0,\text{B32}}}^{E_{F,\text{B32}}} N_{\text{B32}}(E) \, E \, \mathrm{d}E , \tag{12}$$

where N_{B2} and N_{B32} are the density of states for the B2 and the B32 structure, respectively, calculated for the same muffin-tin potential but for different structure factors [12, 32, 33]. $E_{0,\text{B2}}$ and $E_{0,\text{B32}}$ are the energy values of the bottom of the valence bands and $E_{F,\text{B2}}$ and $E_{F,\text{B32}}$ are the values for the Fermi energies. The Fermi energies are determined from

$$\int_{E_0}^{E_F} N(E) \, \mathrm{d}E = z , \tag{13}$$

where z is the number of valence electrons per unit cell.

Wave functions

The wave functions ψ_i are linear combinations of the relativistic augmented plane waves $\varphi_{j,m}$ [18]:

$$\psi_i = \sum_{j,m} c_{j,m} \varphi_{j,m} , \tag{14}$$

$$\varphi_{j,m} = \sum_{\varkappa,\mu} A^{j,s}_{\varkappa,\mu,m} \begin{pmatrix} g^{(s)}_{\varkappa}(r) & \chi^{\mu}_{\varkappa} \\ i f^{(s)}_{\varkappa}(r) & \chi^{\mu}_{-\varkappa} \end{pmatrix} \begin{matrix} (\text{inside the} \\ \text{muffin-tin } s), \end{matrix} \tag{15}$$

and

$$\varphi_{j,m} = \begin{pmatrix} \chi^m \\ \boldsymbol{\sigma} \boldsymbol{k}_j \chi^m \end{pmatrix} \exp\{i \boldsymbol{k}_j \boldsymbol{r}\} \begin{matrix} (\text{outside the} \\ \text{muffin-tins}). \end{matrix} \tag{16}$$

The $\chi^{\mu}_{\varkappa}$ are the spin-angular functions [34] and the χ^m are the spin functions. For the SCF calculations in this paper the spin-angular part of the wave func-

tions is simplified by using relativistic spin wave functions [23]. Within this approximation the large component of the basis function is given by

$$g_{\varkappa}^{(s)} \chi_{\varkappa}^{\mu} \approx g_{l}^{(s)} Y_{l,m_l} \chi^{m} . \tag{17}$$

Then the spin quantum numbers m of the electron states are good quantum numbers and the wave function can be described by the wave vector $\boldsymbol{k}$, the band index n, and m. Inside the muffin-tin spheres the wave functions are expanded in spherical harmonics Y_{l,m_l}, and therefore the charge can be easily separated in s-, p-, and d-like charges. Except for LiZn the major contributions to the charge are of s- and p-like character for all B32 phases investigated here.

Electronegativities

On the basis of the character of the charge inside the muffin-tin spheres we have deduced electron configurations for atomic valence states. It is assumed that appropriate atomic valence configurations for the formation of B32 phases can be described by partial occupation numbers n_s and n_p of s and p atomic orbitals. n_s and n_p are chosen in such a way, that $n_s + n_p$ gives the number of valence electrons of the atomic system (neutral atom or ion, see below), and that the ratio n_p/n_s is the same as found in the intermetallic compound:

$$n_s + n_p = N_{val} , \tag{18}$$

$$r_{met} = n_p/n_s . \tag{19}$$

For these valence states the electronegativities χ are calculated according to the method of Mulliken [35], where χ is defined as the sum of the ionization potential I and the electron affinity A. Contrary to the conventially adopted orbital picture, however, I and A are calculated by the differences

$$A = E^{A} - E^{0} , \tag{20}$$

$$I = E^{0} - E^{K} , \tag{21}$$

where E^{A}, E^{K} and E^{0} are the total energies of the anion, cation and neutral atom, respectively. Then the electronegativity is given by

$$\chi' = A + I = E^{A} - E^{K} \tag{22}$$

or, to obtain values which are close to the Pauling scale [15]

$$\chi = 0.19 \left(\frac{A + I}{e\,V} - 1 \right) e\,V . \tag{23}$$

In the present work E^{A} and E^{K} are calculated by the density functional expression for the total energy, see (1)–(5). For the valence electron configurations, however, the charge density, (5), is chosen as

$$\varrho(\boldsymbol{r}) = \sum_{i} n_i \mid \psi_i(\boldsymbol{r}) \mid^2 , \tag{24}$$

where the occupation numbers n_i are not equal to 1 for the valence electrons, instead the n_i are taken from (18)–(19). The details of the calculation are given elsewhere [16].

Numerical details of the band structure calculations

In this subsection the input data for the SRAPW calculations are listed. For the SCF calculation the valence electrons and the d-electrons (3d-electrons for Zn and Ga and 4d-electrons for Cd and In) are treated as band electrons, that is these electrons are included in the SCF calculation, whereas the other electrons are treated as core electrons. The lattice data are summarized in Table 1. The muffin-tin radii are always taken as approximately half the nearest neighbour distance.

The unit cell used for the calculations is one fourth of the fcc unit cell given in Fig. 1 with two formula units LiMe. The $\boldsymbol{k}$-points, for which the SCF calculation have been performed, have been chosen equidistant in $\boldsymbol{k}$-space. Most calculations have been done for 89 $\boldsymbol{k}$-points in 1/48th of the Brillouin zone. Integration over $\boldsymbol{k}$-space has been performed by extending the tetrahedron method of Lehmann and Taut [36] to volume integrals.

The majority of the calculations has been done with a maximum angular momentum $l_{max} = 5$. The number of RAPW basis functions is chosen according to the Switendick criterion [37] $S = 5$ (about 60 reciprocal lattice vectors $\boldsymbol{k}_j$).

Table 1. Input data for the band structure calculations in atomic units.

Compound	Lattice constant a	Radius of the muffin-tin spheres	Volume of the muffin-tin spheres
LiAl	12.019	2.586	72.41
LiZn	11.733	2.460	62.33
LiGa	11.707	2.460	62.33
LiCd	12.636	2.718	84.13
LiIn	12.823	2.718	84.13

3. Results

Band structure

The resulting band structure and the density of states (DOS) of the valence electrons are shown in Figures 2–6. Except in the case of LiZn these bands do not overlap with the lower lying d-like bands. The energetic separations E_{ds} between the d-like bands and the valence bands are given in Table 2. The values of E_{ds} are correlated to the delocalization of the electronic states of the d-bands. This can be seen from the values of the amount of charge of the d-band electrons inside a sphere centered at the Li nuclei, which are also listed in Fig. 2 (for LiZn, for which the d-bands overlap with the valence bands, the d-band contribution is defined as the contribution of the lowest 10 electronic states for each $\boldsymbol{k}$-point).

As can be seen from Figs. 2–6, the band structure and density of states curves of the valence electrons are very similar for all compounds LiMe. The various valence bands are narrow and almost separated from each other. These narrow bands are typical for the B32 structure. The bands in the B2 structure are broader than in the B32 structure and the different bands show more overlap. In Fig. 7 the density of states of LiCd is plotted for the B32 and the B2 structures. Because of the larger overlap of the bands in the B2 structure, the strong decrease of the DOS between the 4th and 5th band is missing in the B2 structure. The extremely narrow bands of the LiMe B32 compounds cause the unusual magnetic properties of these alloys.

In addition to the total DOS the local densities of states [38]

$$q_s(E) = N(E) \int_{\omega_s} \varrho(\boldsymbol{r}, E)\, \mathrm{d}\tau\,; \quad s = \mathrm{Li}, \mathrm{Me} \quad (25)$$

are shown in Figures 2–6. $\varrho(\boldsymbol{r}, E)$ is the electron density of the states with energy eigenvalue E, $N(E)$ is the DOS and ω_s is the volume of the muffin-tin sphere s. From the curves $q_s(E)$ vs. E one can see that there is a significant difference between the charge distribution of the lower two valence bands and the upper valence-conduction bands (3rd to 6th bands). For the lower bands $q_{Me}(E)$ is much larger than $q_{Li}(E)$, that is the charge for these states is more or less concentrated on the non-Li spheres. For the upper valence bands the electronic charge is much more evenly distributed.

Table 2. Distances E_{ds} between the top of the d-like bands and the bottom of the valence bands in the B32 phases LiMe. The electronic charge of the d-band electrons Q_R inside a sphere of radius $R = 2.46\, a_0$ around the Li nuclei is given too.

Compound	E_{ds}/eV	Q_R/e^-
LiZn	0	0.081
LiCd	0.56	0.040
LiGa	4.56	0.012
LiIn	4.98	0.011

The resulting character of the chemical bond can be seen in Fig. 8, where contour maps of the charge density ϱ are plotted for the (101)-plane for the first and fourth valence bands of LiIn. The charge density contour lines are normalized to a constant charge density $\varrho_0 = 1/\omega$.

From Fig. 8 one can see that the electronic states in the first valence band contribute to strong covalent bonds formed by the diamond-like sublattice of the non-alkali metal. A similar result is found for the second band. For the states of the upper bands, like the fourth band shown in Fig. 8c the electronic distribution is more metal-like. This metallic character is indicated in Fig. 8 by the two facts that a) the electron density in the bond directions is less pronounced in comparison to the first band and b) the corresponding charge is more uniformly distributed. Between the Li atoms, however, ϱ is distinctly smaller than ϱ_0, whereas $\varrho > \varrho_0$ between the In atoms. Furthermore, one finds a gradient in the charge density in the region between the In and the Li atoms. This can be also seen from Fig. 9, where the total charge density of the valence electrons of LiIn is plotted in the [111] direction. It is interesting to note that the charge density between the Li atoms differs significantly for the various alloys. This can be seen from Fig. 10a, where the charge densities of the valence electrons in the [111] direction between the Li atoms are plotted for LiAl and LiIn. In Fig. 10b a comparison is made between the electron density gained from the band structure calculation and the electron density which one gets from overlapping atomic charge densities.

The charge distributions are given quantitatively in Table 3. In addition to the total amount of charge Q_s (s = Li, Al, ...) inside the muffin-tin spheres, the amount of charge for the first two bands is listed, as the ratio Q_{Li}/Q_{Me} yields some information about the bonding character, see above. To study trends in the

charge transfer, also the amount of charge inside a Li-sphere of radius $R = 2.46\,a_0$, $Q_{R,B32}$, is given. Besides the band structure result $Q_{R,B32}$, the charge which one gets from overlapping atomic charge densities, $Q_{R,A0}$, is calculated. The differences $Q_{R,B32} - Q_{R,A0}$ are listed in Table 3 too (3rd row from the bottom). The radius of $R = 2.46\,a_0$ has been taken, because this is the muffin-tin radius for LiZn and LiGa and because $2.46\,a_0$ is approximately equal to the covalent bonding radius of Li. The charge transfers are given only for the Li spheres, because the gain in charge for the "anionic" sublattice is not located inside the atomic spheres, but is spread out over the whole region of this sublattice, see Figure 8. Finally, the ratio r_{met}, (19), of the p- to s-like charges inside the muffin-tin spheres is listed in the last row of Table 3.

Finally, in Table 4 the differences in the ordering energies ΔE for LiMe are shown. The compound LiZn is omitted in this Table because for this phase the valence electron bands overlap with the d-like bands of Zn, see above. One can see from Table 4 that ΔE is positive for all alloys and that the electronic band structure energies favour the B32 structure. In Fig. 11 the difference in the ordering energy is plotted as a function of the upper limit of the integral in (12). Because the Fermi energy is a function of the number of valence electrons (NOVE) per formula unit LiMe, see (13), ΔE can be displayed directly as a function of the NOVE. The data given

Table 3. Charge distribution of the valence electrons in B32 phases LiMe.

	Atomic sphere	Compound LiMe				
		LiZn	LiCd	LiAl	LiGa	LiIn
Total valence electron charge inside the muffin-tin spheres given in Table 1	Li	0.504	0.640	0.717	0.589	0.658
	Me	1.441	1.346	1.954	1.979	1.928
Charge of 1st and 2nd band inside the muffin-tin spheres	Li	0.247	0.335	0.286	0.203	0.225
	Me	1.086	0.983	1.088	1.158	1.140
Valence electron charge inside atomic Li-spheres with radii $R = 2.46\,a_0$	Li	0.504	0.436	0.587	0.589	0.440
Charge transfer for the Li-sphere with $R = 2.46\,a_0$	Li	−0.051	−0.014	−0.066	−0.083	−0.078
p- to s-like charge r_{met} inside the muffin-tin spheres	Li	1.74	1.50	1.81	1.87	1.72
	Me	0.78	0.71	1.17	0.89	0.94

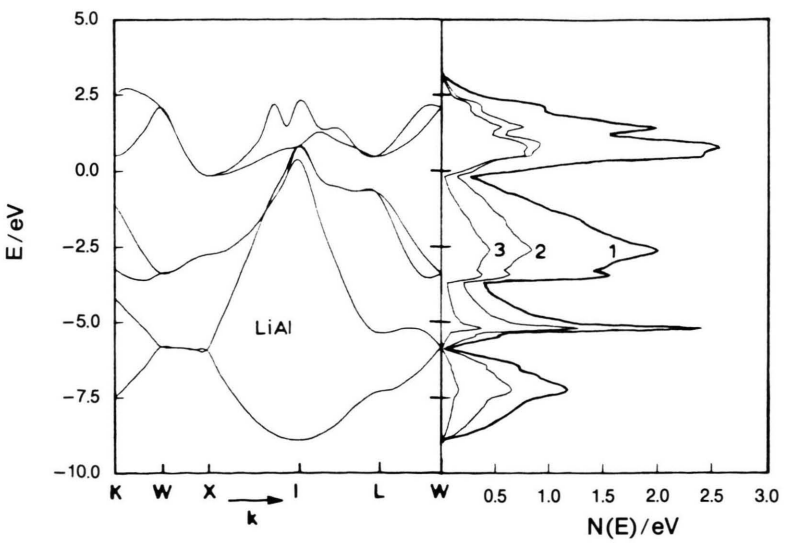

Fig. 2. Left: Band structure of the first six valence bands of LiAl. The zero of the energy scale is the Fermi energy E_F. – Right: Density of states (DOS) $N(E)$ for the electronic bands show on the l. h. s. Curve 1: total DOS per unit cell; curve 2: partial DOS q_{Al} for the Al sphere; curve 3: partial DOS q_{Li} for the Li sphere.

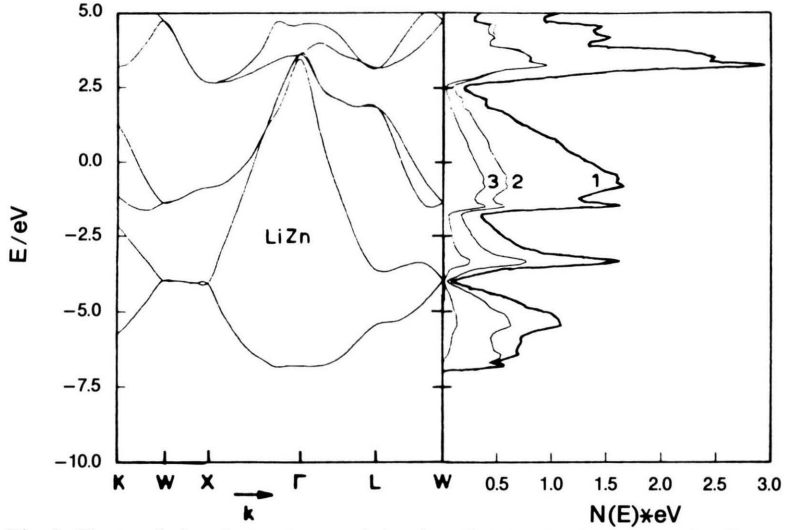

Fig. 3. Electronic band structure and density of states for LiZn. For details see legend to Figure 2.

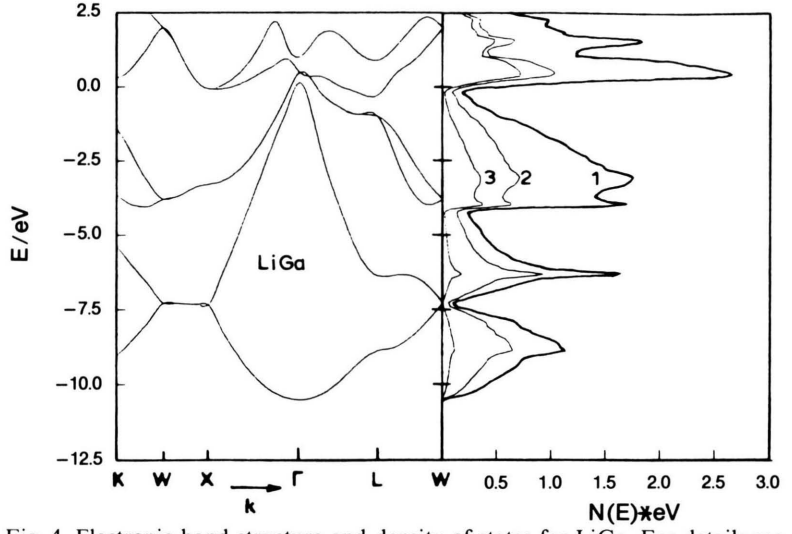

Fig. 4. Electronic band structure and density of states for LiGa. For details see legend to Figure 2.

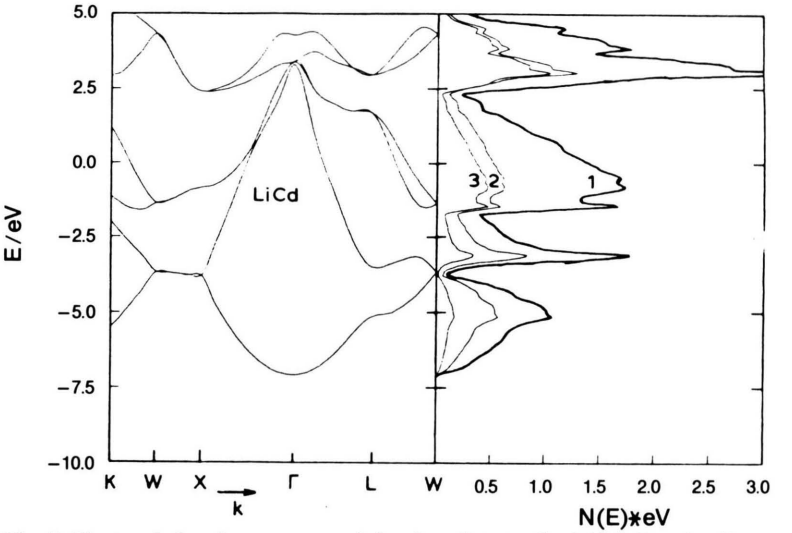

Fig. 5. Electronic band structure and density of states for LiCd. For details see legend to Figure 2.

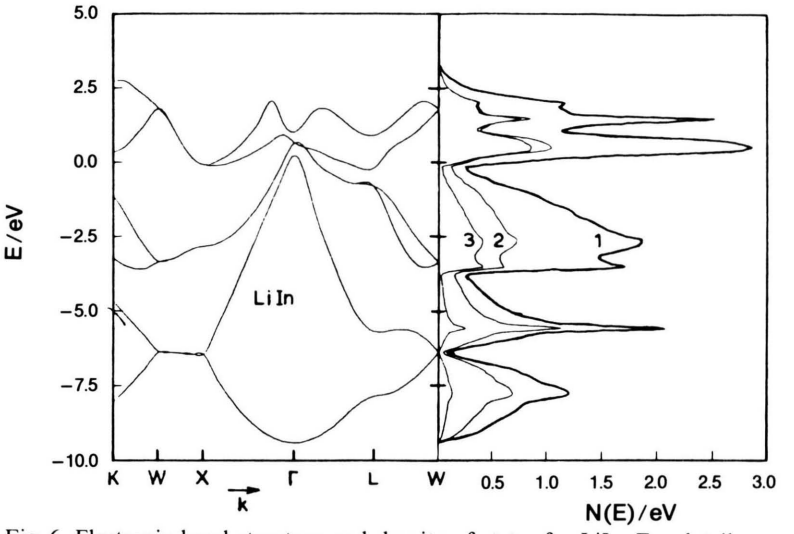

Fig. 6. Electronic band structure and density of states for LiIn. For details see legend to Figure 2.

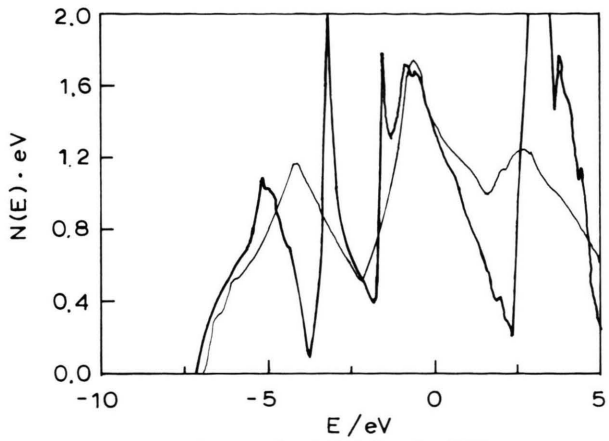

Fig. 7. Density of states for LiCd for the B32-type structure (thick line) and for the B2-type structure (thin line). The calculations have been performed for lattice constants $2a\,(B32) = a\,(B2)$.

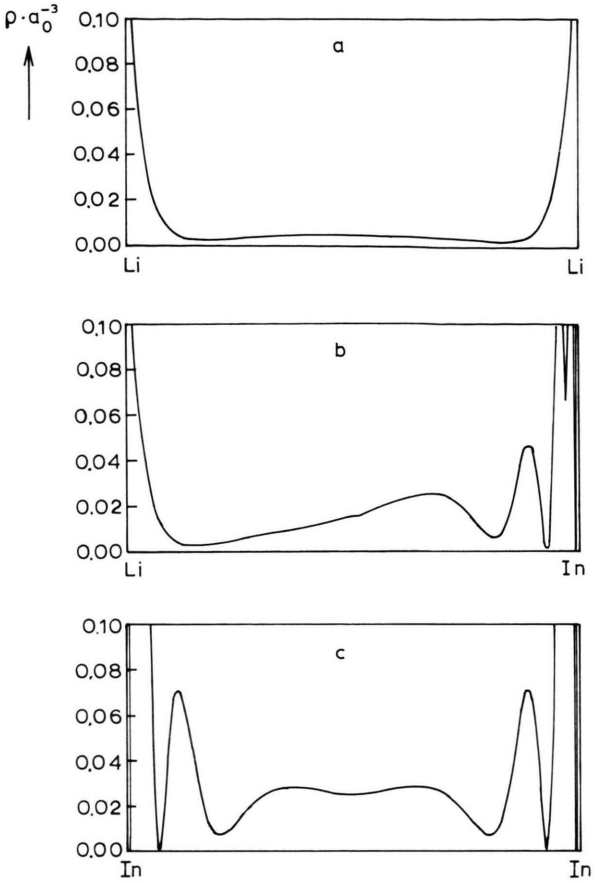

Fig. 9. Charge density ϱ for the valence states of LiIn for the (111) direction. ϱ is plotted from one nucleus site to the next nucleus site.

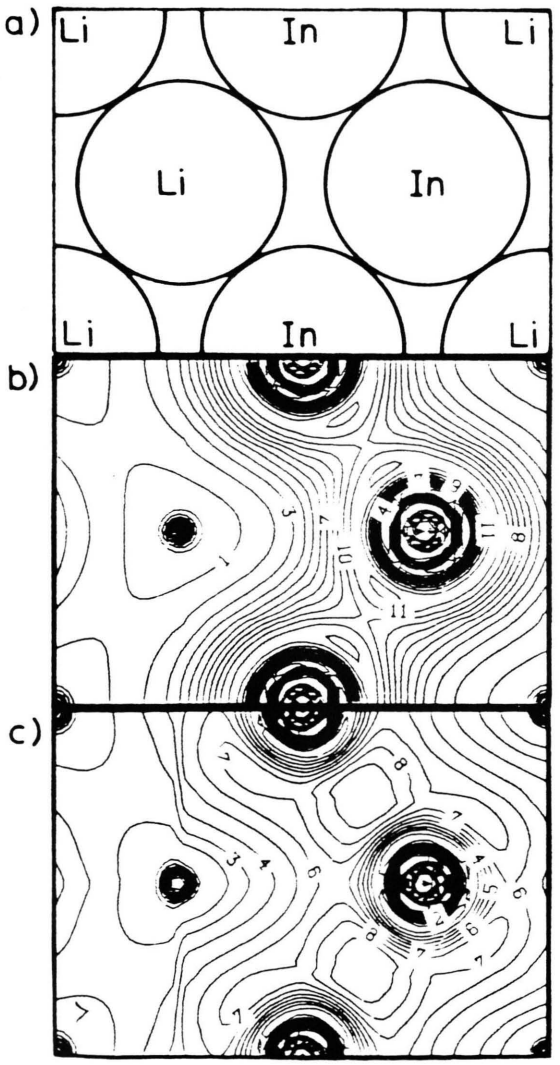

Fig. 8. Display of contour lines of the charge density ϱ for the (101) plane for LiIn. The numbers at the contour lines correspond to the normalization $\varrho' = 5\varrho/\varrho_0$ where ϱ_0 is equal to the constant distribution of one electron; $\varrho_0 = 1/\omega$. It follows that the contour line with $\varrho = \varrho_0$ is labeled by the number 5. a) Atomic positions in the (101) plane. b) Contour lines for the mean of the electron states of the 1st valence band. c) Contour lines for the mean of the electron states of the 4th valence band.

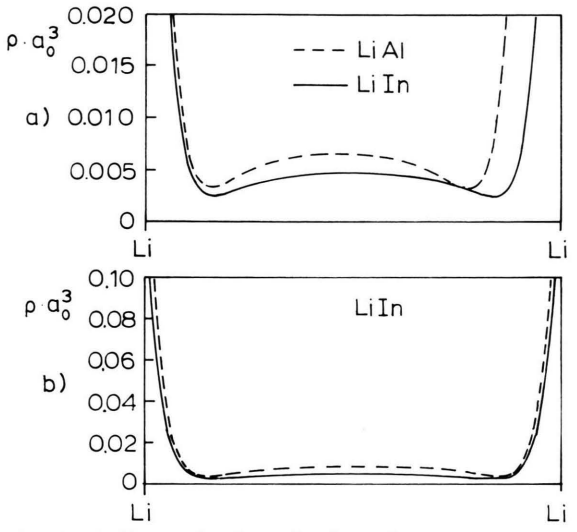

Fig. 10. a) Charge density ϱ for the valence states of LiIn and LiAl between two neighboured Li atoms. b) Charge density ϱ for the valence states of LiIn between two neighboured Li atoms. The full lines show the band structure result whereas the dotted lines give the result from overlapping the charge densities of the free atoms Li and In.

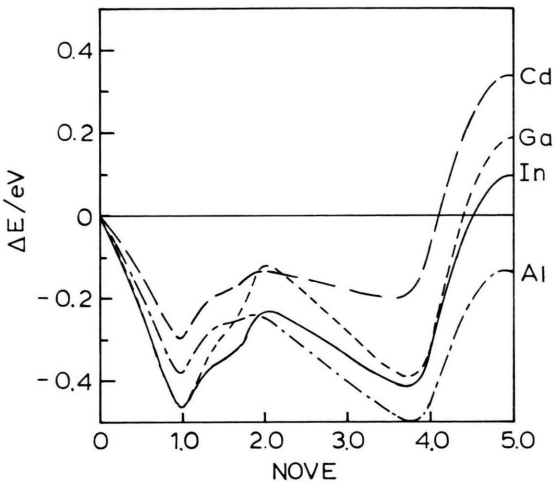

Fig. 11. Differences in the ordering energy $\Delta E = E(B32) - E(B2)$ as a function of the number of occupied states (number of valence electrons per half unit cell (NOVE)) for compounds LiMe (Me = Al, Ga, Cd and In). For stoichiometric LiMe the NOVE is equal to 3 (LiCd) or 4.

Table 4. Differences in the ordering energy $\Delta E = E(B2) - E(B32)$ per formula unit LiMe for compounds LiMe. The calculations have been performed for lattice constants $a(B32) = 2a(B2)$ using the muffin-tin potential of the SCF calculation for the B32 structure.

Compound	ΔE/eV
LiAl	0.444
LiGa	0.322
LiCd	0.182
LiIn	0.335

Table 5. Atomic electronegativities χ.

Atom	Valence configuration	Present work	Pauling[1]	Atomic ground state[2]
		χ [eV]	χ [eV]	χ [eV]
Li	$2s^{0.4}\ 2p^{0.6}$	0.65	1.0	1.00
Al	$3s^{1.5}\ 3p^{1.5}$	2.00	1.5	1.00
Zn	$4s^{1.2}\ 4p^{0.8}$	1.85	1.6	
Ga	$4s^{1.5}\ 4p^{1.5}$	2.28	1.6	1.06
Cd	$4s^{1.2}\ 4p^{0.8}$	1.74	1.7	
In	$5s^{1.5}\ 5p^{1.5}$	2.13	1.7	1.03

[1] Ref. [15], [2] Ref. [39].

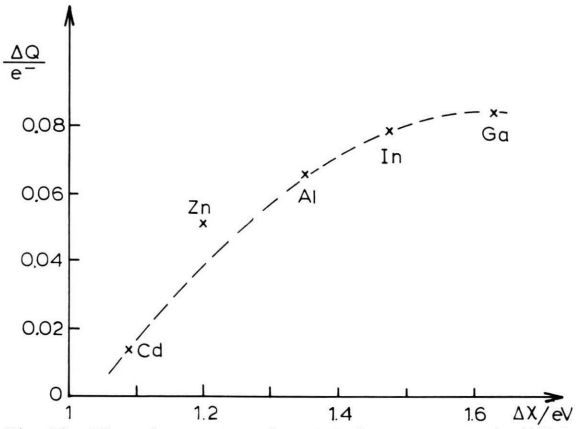

Fig. 12. The charge transfer ΔQ for compounds LiMe (Me = Al, Zn, Ga, Cd and In) as a function of the differences in the electronegativities $\Delta\chi = \chi(Me) - \chi(Li)$.

in Table 4 are the values for NOVE = 3 or 4, respectively.

Electronegativities

The results of the calculation of the electronegativities χ are given in Table 5. For comparison the values of χ from Pauling [15] and the values which one gets for the atomic ground states [39] are listed too. The valence electron configurations for which χ is calculated are deduced from the data of the last row of Table 3. For the trivalent atoms Al, Ga and In r_{met} is roughly 1, whereas for Zn and Cd r_{met} is close to 2/3. Therefore these values are used in our calculations. For lithium r_{met} from Table 3 is

1.7, from which one gets approximately the valence electron configuration $2s^{0.4}2p^{0.6}$.

In Fig. 12 the charge transfer found for the LiMe systems, see Table 3, is plotted as a function of the differences in the electronegativities of the atoms. One can see from Fig. 12 that, although one does not obtain a straight line, $\Delta\chi$ and ΔQ show the same trend. Table 5 also demonstrates that electronegativities calculated for ground states are not as useful as those calculated for valence states.

4. Discussion

The band structure results given in the previous section show that the electronic structure of all binary B32 phases LiMe (Me = Al, Zn, Ga, Cd and In) are very similar. The width of the dispersions is smaller and the different bands show less overlap than expected for intermetallic phases. It is remarkable that only a small charge transfer $\Delta Q/Q$ of about 10% from the Li atoms to the other metal atoms is found. Therefore charge transfer seems not to be of special importance for the occupation dependence for the chemical bonds. The model that the Me sublattice forms saturated sp^3 hybrid states by getting one electron from the Li could not be confirmed. These findings are in accordance with earlier investigations on LiAl [24, 40].

From the Figs. 2–6 and 8 as well as from the charge distribution given in Table 3, one concludes that the bonding character is a superposition of covalent and metallic contributions with a small ionic component.

This small ionic contribution to the chemical bond occurs between the Li- and the Me^{II}/Me^{III}-sublattice, as a result of the small charge transfer from the Li to the Me atoms. The reduction of charge in the Li sublattice is mainly restricted to the region near the Li-Li direction, as can be seen from Figure 10b. From this reduction of charge in the Li-Li direction a nonbonding contact of the Li atoms result, which is found in other Zintl phases too [40, 41]. The Li-$Me^{II,III}$ interaction is both slightly ionic as mentioned above as well as covalent/metallic as the Me-Me contacts. The interplay of metallic and covalent bonding mechanisms will be discussed in more detail next.

For the electronic states of the lower two valence bands (1st and 2nd bands in the Figs. 2–6), one finds strong covalent bonds mainly localized in the Me^{II}/Me^{III} sublattices. The electronic charge distribution for these bands (see the electronic charge density contour lines in Fig. 8b) is similar to the electronic charge distribution in diamond-like semiconductors. The 1st band is nearly a pure s-like band, whereas the 2nd is an s-p-hybrid. Summing over these two bands one gets 70–80% s-character. Only for LiIn the p-character is larger. Therefore the two lower valence bands are of covalent nature and are formed mainly by the outermost s electrons of the Me^{II}/Me^{III} atoms.

Above these bands there are two strongly overlapping dispersions (3rd and 4th bands in Figures 2–6). They are occupied valence bands for the LiMe compounds and half filled ones for the LiMe alloys. For the electronic states of these bands the covalent character is less pronounced than for the 1st and 2nd bands. The electronic charge is more spread over the whole crystal and the valence electrons of the Li atoms are more involved in the chemical bond, as can be seen from the example give in Figure 8b and c. One can conclude that for the electronic states of the 3rd and 4th bands the Li-Me and Me-Me contacts are more metallic-like than the Me-Me contacts of the 1st and 2nd band. The relative contribution of metallic and covalent interaction with the bond, however, can not be given from these investigations.

The non-occupied 5th and 6th bands are predominantly metal-like, that is the charge of the electronic states of these bands is more or less uniformly distributed over the whole crystal. This is indicated in the Figs. 2–6 by the values of the partial densities of states $q_{Li}(E)$ and $q_{Me}(E)$, namely the ratio q_{Li}/q_{Me} is close to 1.

Next the correlation between the charge transfer ΔQ and the electronegativities $\Delta\chi$ shall be discussed. Our concept of calculating atomic electronegativities χ for atomic valence configurations seems to be a useful one, as the differences in χ correlate with the magnitude of the charge transfer. On the other side, the calculated charge transfer is extremely small, as found for LiAl by other authors [24, 40]. To investigate whether or not the correlation between ΔQ and $\Delta\chi$ is of physical significance, another measure of the charge transfer is taken. ΔQ is calculated by the same procedure as explained in the previous section; for the volume of integration, however, we have taken a narrow cone in the Li-Li nearest neighbours direction instead of a sphere. As can be

deduced from the charge densities displayed in Fig. 10, the charge transfer $\Delta Q_{cone} = Q_{B32,cone} - Q_{A0,cone}$ is of the same order of magnitude as $Q_{B32,cone}$ itself. Plotting ΔQ_{cone} as a function of $\Delta\chi$, one gets the same trend as displayed in Figure 12. Therefore we assume that the charge transfer from the Li sublattice to the Me^{II}/Me^{III} sublattice follows from the differences in the electronegativities of the components of the compounds LiMe. However, a simple correlation between electronegativities and charge transfer can not be found generally for intermetallic compounds. For example calculating the charge transfer for the B2 phase LiTl in the same manner as explained in the previous section, the charge transfer is much smaller than expected from the values of the electronegativities. Also for the hypothetic B2 phase LiIn, one gets no charge transfer.

Next some remarks shall be made on LiZn. In LiZn the 3d and the valence bands overlap and in the overlap-region one gets s-d-hybrid states. This overlap makes it difficult to define the valence state properly, because there is no unique way to include the d-character. Therefore the influence of the 3d electrons on χ can not be given quantitatively. A model calculation, however, assuming a valence electron configuration $3d^1 4s^{0.4} 4p^{0.6}$, that is taking one of the ten 3d electrons as a valence electron, increases the value of χ drastically from $\chi = 1.85$ eV (see Table 5) to $\chi = 2.72$ eV. Therefore a 3d valence electron might increase the charge transfer from lithium to zinc. This might explain why the value for Zn in Fig. 12 is to the left of the hatched line. There is, however, another charge transfer effect of the d electrons. It is found for molecules that inner d electrons have the tendency to delocalize over the neighbouring atomic sites [42]. A similar effect is found for the phases studied here. This can be seen most clearly for those compounds, for which the d and valence electron bands are separated by a band gap. For LiCd, for example, the total amount of charge of the 4d electrons within the Li sphere is equal to $Q_{4d,B32} = 0.073\ e^-$, whereas from overlapping atomic charge densities on gets only $Q_{4d,A0} = 0.039\ e^-$.

Next it shall be discussed whether or not one finds a correlation between the Li-Li bond distances and the charge distribution within the Li-Li sublattice. Schäfer et al. [4] found a relation between the electronegativity and the bond distance for some Si containing Zintl-phases in the sense that graduations in the charge transfer for different compounds influence the bond lengths because of the change of the Coulomb repulsion of the ions. Comparing the lattice constants (Table 1) and the electronegativities (Table 5) such a correlation can not be found for the compounds considered here. The reason might be that the small charge transfer found for these phases is of minor importance for the interplay of charge distribution and bonding distances. On studying for example the data given in Table 3 in the 3rd and 4th row from the bottom, one observes that the charge transfer is much smaller than the differences in the total charges in the Li-Li region for different compounds. There is, however, a distinct trend if one compares the total charge (charge of the valence and the d electrons) in the Li sphere with radius $R = 2.46\ a_0$ with the lattice constant. If one adds the values for the charge from Table 2 (last column) and from Table 3 (4th row from the bottom), one gets decreasing values for the charge with increasing lattice constants. However for LiZn and LiAl one observes nearly the same amount of charge, although the lattice constants are distinctly different. Two problems occur in quantifying the results from the present work. Firstly, there is some ambiguity to define the "region of the Li sublattice". Secondly, only the spherical mean of the charge is calculated here. A detailed analysis of the anisotropy of the charge distribution in the bonding region might give more insight into a possible correlation between the charge distribution and the equilibrium distances.

Finally, the differences in the band structure of the B2 and the B32 structures shall be discussed. Comparing the Figs. 7 and 11 one can conclude that for a number of valence electrons per formula unit LiMe smaller than 5 the narrow bands of the B32 structure would be favoured from the energetic point of view. As pointed out earlier [12], this only holds for systems for which the sizes of the atoms are identical.

[1] E. Zintl, Angew. Chem. **52,** 1 (1939).
[2] W. Klemm, Proc. Chem. Soc. London **1958,** p. 329.
[3] H. Schäfer and B. Eisenmann, Rew. Inorg. Chem. **3,** 29 (1981).
[4] H. Schäfer, B. Eisenmann, and W. Müller, Angew. Chem. **85,** 742 (1973); Angew. Chem. Int. Ed. Engl. **12,** 694 (1973).
[5] E. Moser and W. B. Pearson, Phys. Rev. **101,** 1608 (1956).
[6] H. G. von Schnering, Angew. Chem. **93,** 44 (1981); Angew. Chem. Int. Ed. Engl. **20,** 33 (1981).
[7] W. Klemm and H. Fricke, Z. Anorg. Allg. Chem. **282,** 162 (1955).
[8] R. E. Watson, L. H. Bennett, G. C. Carter, and I. D. Weisman, Phys. Rev. B**3,** 222 (1971).
[9] G. Grube and A. Schmidt, Z. Elektrochem. **42,** 201 (1936).
[10] G. Grube, H. Voßkühler, and H. Vogt, Z. Elektrochem. **38,** 869 (1932).
[11] P. W. Anderson, Conceps in Solids, Benjamin, New York 1963, p. 6; L. Brewer, High Strength Materials, Ed. V. Zackay, John Wiley, New York 1964, p. 37. – N. Engel, Developments in the Structural Chemistry of Alloy Phases, Ed. B. Giessen, Plenum Press, New York 1969, pp. 25–40. – W. Hückel, Structural Chemistry of Inorganic Compounds, Elsevier, Amsterdam 1951, pp. 829ff.
[12] P. C. Schmidt, Phys. Rev. B, in press.
[13] A. B. Makhnovetskii and G. L. Krasko, phys. stat. sol. (b) **80,** 341 (1977).
[14] M. B. McNeil, W. B. Pearson, L. H. Bennett, and R. E. Watson, J. Phys. C **6,** 1 (1973).
[15] L. Pauling, Nature of the Chemical Bond, 3rd ed. Cornell University Press, Ithaca, New York 1960, pp. 88–93.
[16] M. C. Böhm and P. C. Schmidt, to be published.
[17] J. Hinze and H. H. Jaffe, J. Amer. Chem. Soc. **84,** 540 (1962).
[18] T. Loucks, Augmented Plane Wave Method, Benjamin, New York 1967; J. O. Dimmock, Sol. State Physics **26,** 104 (1971).
[19] P. Hohenberg and W. Kohn, Phys. Rev. **136,** B864 (1964).
[20] J. C. Slater, J. Chem. Phys. **57,** 2389 (1972).
[21] J. F. Janak, Phys. Rev. B **9,** 3985 (1974).
[22] A. H. MacDonald and S. H. Vosko, J. Phys. C **12,** 2977 (1979).
[23] D. D. Koelling and B. N. Harmon, J. Phys. C **10,** 3107 (1977).
[24] T. Asada, T. Jarlborg, and A. J. Freeman, Phys. Rev. B **24,** 510 (1981) and 857 (1981).
[25] M. Zwilling, P. C. Schmidt, and Alarich Weiss, Appl. Phys. **16,** 255 (1978).
[26] W. Kohn and L. J. Sham, Phys. Rev. **140,** A1133 (1965).
[27] J. C. Slater, Phys. Rev. **81,** 385 (1951).
[28] L. Hedin and S. Lundqvist, J. de Physique C **3,** 73 (1972).
[29] U. von Barth and L. Hedin, J. Phys. C **5,** 1629 (1972).
[30] S. H. Vosko, L. Wilk, and M. Nusair, Can. J. Phys. **58,** 1200 (1980).
[31] J. C. Slater and P. de Cicco, MIT Report (1964, unpublished).
[32] V. Heine, Sol. State Physics **35,** 1 (1980).
[33] D. G. Pettifor, J. Phys. C **3,** 367 (1970).
[34] E. M. Rose, Relativistic Electron Theory, John Wiley, New York 1961.
[35] R. S. Mulliken, J. Chem. Phys. **2,** 782 (1934); **3,** 573 (1935).
[36] G. Lehmann and M. Taut, phys. stat. sol. (b) **54,** 469 (1972).
[37] L. F. Mattheiss, J. H. Wood, and A. C. Switendick, Methods in Computational Physics **8,** 64 (1968).
[38] J. Friedel, Adv. Phys. **3,** 446 (1954).
[39] P. C. Schmidt and M. C. Böhm, Ber. Bunsenges. Phys. Chem. **87,** 925 (1983).
[40] A. Zunger, Phys. Rev. B **17,** 2582 (1978).
[41] R. Ramirez, R. Nesper, H.-G. von Schnering, and M. C. Böhm, Chem. Phys., in press.
[42] M. C. Böhm and R. Gleiter, J. Oranomet. Chem. **228,** 1 (1982).